# Journal of Materials Chemistry C

Accepted Manuscript

This article can be cited before page numbers have been issued, to do this please use: K. Li, J. Fan, M. Shang, H. Lian and J. Lin, *J. Mater. Chem. C*, 2015, DOI: 10.1039/C5TC01993A.

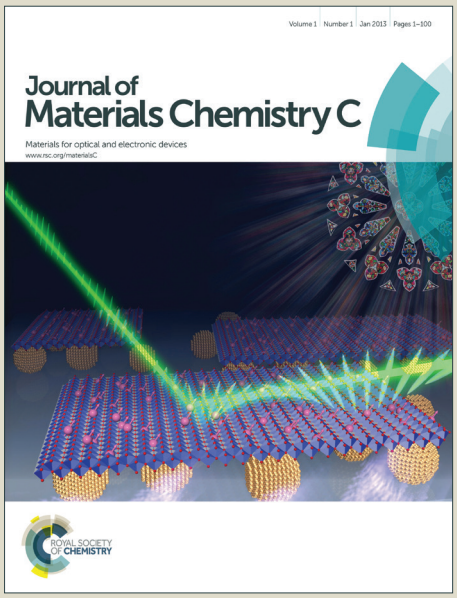




ROYAL SOCIETY OF CHEMISTRY

www.rsc.org/materialsC

View Article Online
DOI: 10.1039/C5TC01993A

Journal of
Materials Chemistry C

ARTICLE

# $Sr_2Y_8(SiO_4)_6O_2:Bi^{3+}/Eu^{3+}$: a single-component white- emitting phosphor via energy transfer for UV w-LEDs

Received 00th January 20xx,
Accepted 00th January 20xx

DOI: 10.1039/x0xx00000x

www.rsc.org/

Kai Li,[ab] Jian Fan,[a] Mengmeng Shang,[a] Hongzhou Lian*[a] and Jun Lin*[a]

A series of $Bi^{3+}$, $Eu^{3+}$-doped $Sr_2Y_8(SiO_4)_6O_2$ (SYSO) phosphors were synthesized by the Pechini-type sol-gel route. XRD patterns and Rietveld refinement, FT-IR spectra, photoluminescence spectra (PL), fluorescent decay times, quantum yields (QYs) were utilized to characterize the as-prepared samples. Intense blue-green emission due to the $^3P_1 \rightarrow {}^1S_0$ transition of $Bi^{3+}$ ions is produced under UV excitation in $Bi^{3+}$ singly-doped SYSO samples. Spectral analysis illustrates that two kinds of $Bi^{3+}$ are generated by occupying the two kinds of sites (4f and 6h) available for Y in SYSO, denoted as $Bi^{3+}(1)$ and $Bi^{3+}(2)$, corresponding to the two main emission bands around 413 and 493 nm, respectively. Wide spectral overlap between $Bi^{3+}$ emission and $Eu^{3+}$ excitation spectra results in the energy transfer from $Bi^{3+}$ to $Eu^{3+}$. This has been demonstrated via the excitation spectra monitored at $Bi^{3+}$ and $Eu^{3+}$ emission bands, and the PL emission spectra and decay times of $Bi^{3+}$ in SYSO: $Bi^{3+}$, $Eu^{3+}$ phosphors. The energy transfer mechanism is determined to be dipole-quadrupole interaction. The critical distance of energy transfer from $Bi^{3+}$ to $Eu^{3+}$ ions is calculated to be 12.78 Å based on the concentration quenching method, which is in good agreement with that of spectral overlap route (10.03-13.37 Å). Moreover, the QYs, CIE chromaticity and thermal quenching properties have also been investigated. White emission color can be realized with the CIE coordinates (0.325, 0.311) and QY 52% for SYSO:0.08$Bi^{3+}$, 0.48$Eu^{3+}$. The above results suggest that SYSO:$Bi^{3+}$, $Eu^{3+}$ can be of potential as a single-component white-emitting phosphor for UV w-LEDs.

## 1. Introduction

Recently, white-light-emitting diodes (w-LEDs), a next-generation of illumination source, have been drawing worldwide attention due to their superior advantages such as low power consumption, long operation lifetime, good stability in physical and chemical properties and especial mercury-free properties, which are considered to be the excellent candidates to replace the current conventional fluorescent and incandescent lamps.[1] It is well known that the most effective white lighting device can be realized by combining a blue-emitting LED chip with yellow-emitting YAG:$Ce^{3+}$ (excited by blue light) phosphors. This kind of phosphor-converted w-LED fabrication involves some advantages such as low cost, a single-chip fabrication process, and circuit simplicity.[2] Regretfully, this method exhibits a poor color-rendering index (CRI) and a high correlated color temperature (CCT) attributed to the deficiency of red component for warm white light, which constricts its application for indoor lighting. Another useful way is suggested to improve this issue by employing near-ultraviolet (n-UV)/UV LED chips with red, green, and blue phosphors. However, there exist the problems of trade-off luminescent efficiency (originating from the reabsorption of blue-emission by the green and red phosphors) and high expenses. Besides, different attenuation situations of each phosphor will give an unstable white light.[3] Therefore, w-LEDs are proposed to be fabricated by a UV/n-UV LED chip coated with a single-phase white-light-emitting phosphor, which has been an active research topic in solid state lighting field. It is well accepted that energy transfer from sensitizers to acceptors in certain host can play an important role to generate the tunable emission color including white. A large number of single-phase white-light-emitting phosphors suitable for UV-pumped w-LEDs have been reported, most of which are based on $Eu^{2+}$-$Mn^{2+}$, $Ce^{3+}$-$Mn^{2+}$, $Eu^{2+}$-$Tb^{3+}$-$Mn^{2+}$, $Ce^{3+}$-$Tb^{3+}$-$Mn^{2+}$ and $Ce^{3+}$-$Dy^{3+}$ systems[4] because the $Eu^{2+}$ and $Ce^{3+}$ have the high emission intensity and broad band spectra originated from their 4f-5d parity allowed electric dipole transitions, and can effectively transfer their energy to activators to enhance the emission of coactivators.[5] However, the red component from $Mn^{2+}$ 3d-3d transition in $Mn^{2+}$-contained white-emitting systems often presents wide emission range, therefore, the color purity of red section is not satisfactory, which may be partly overlapped by some blue and green parts. As we know, $Eu^{3+}$ can yield dominant red emission line due to its electric dipole $^5D_0 \rightarrow {}^7F_2$ transition when it deviates from the inversion center of the crystal lattice. Some efforts have been done to enhance red emission of $Eu^{3+}$ based on the energy transfer effect from $Bi^{3+}$ to $Eu^{3+}$ ions.[6] However, $Bi^{3+}$ can emit the blue-green band emission around 400-550 nm attributed to its 6s6p→6s$^2$ transition, which also can be expected to achieve white light emission when combined with $Eu^{3+}$ red emission (mainly due to their $^5D_0 \rightarrow {}^7F_2$ transition) in single-component phosphor, just like the effect of above systems. Nevertheless, few works have been devoted to this,

[a]State Laboratory of Rare Earth Resource Utilization, Changchun Institute of Applied Chemistry, Chinese Academy of Sciences, Changchun 130022, P. R. China. Email: jlin@ciac.ac.cn (Jun Lin); hzlian@ciac.ac.cn (Hongzhou Lian) Fax: +86-431-85698041; 86-431-85262031
[b]University of Chinese Academy of Sciences, Beijing 100049, P. R. China.

View Article Online
DOI: 10.1039/C5TC01993A




which gives us an inspiration to explore the luminescence properties on the $Bi^{3+}$/$Eu^{3+}$ co-doped phosphors.

Silicate have been extensively investigated as the hosts for rare earth ions incorporation because of their diverse crystal structures and chemical and physical stabilities originated from their strong and rigid frameworks with covalent Si–O bonds which can provide a relatively distorted and complex coordination environment around the cations.[7] Apatite-related silicate compounds, a large family of silicates, have been used as the hosts for phosphors because they can show good photoluminescence (PL) properties when doped with rare earth (RE) ions for solid state lighting.[8] These oxy-apatite host lattices consist of two cationic sites, that is, seven-fold coordinated 6h sites with $C_s$ point symmetry and the nine-fold coordinated 4f sites with $C_3$ point symmetry. Both two sites are demonstrated to be suitable and easily accommodated a great variety of $RE^{3+}$ ions.[9] Recently, Zhou etc.[10] have developed a new single-phased silicate phosphor $MgY_2Si_3O_{10}:Eu^{3+}/Bi^{3+}$, showing tunable emission color containing white light based on the energy transfer (ET) from $Bi^{3+}$ to $Eu^{3+}$. In 2010, Shen etc.[11] have reported the crystal structure and PL properties of $Eu^{3+}$-doped $Sr_2Y_8(SiO_4)_6O_2$, in which a large amount of $Eu^{3+}$ can be introduced into the $Sr_2Y_8(SiO_4)_6O_2$ (SYSO) compound. The structure of SYSO belongs to the apatite style with the space group of $P6_3/m$, where *6h* site are completely occupied by Y2 with seven-fold coordination, while other Sr1 and Y1 are randomly distributed in *4f* site with nine-fold coordination. $Sr_2Y_8(SiO_4)_6O_2:Eu^{2+},Eu^{3+}$ phosphor synthesized and studied by J. Sokolnick etc. produced white light based on the two different sites of Y in this host.[12] As is described above, the introduction of $Bi^{3+}$ into silicate such as SYSO here with two different crystallographic sites may be also highly expected to produce two different emission bands. They can overlap the excitation spectrum of $Eu^{3+}$ and then sensitize it to enhance its emission when $Bi^{3+}$ and $Eu^{3+}$ are co-doped into SYSO compound. Herein, we have successfully synthesized the SYSO:$Bi^{3+}$, $Eu^{3+}$ phosphor via the Pechini-type sol-gel method. As a new single-component tunable emission phosphor SYSO:$Bi^{3+}$, $Eu^{3+}$, the crystal phase, PL properties and Commission Internationale de L'Eclairage (CIE) chromaticity coordinates and quantum yields have been investigated in detail. This phosphor not only shows characteristic $Bi^{3+}$ emission in blue-green area, but also the ET from $Bi^{3+}$ to $Eu^{3+}$ ions. Additionally, the ET mechanism and critical distance from $Bi^{3+}$ to $Eu^{3+}$ ions have been discussed in detail as well.

## 2. Experimental

### 2.1 Materials and Synthetic procedures

$Y_2O_3$ (99.99%) and $Eu_2O_3$ (99.99%) were purchased from Science and Technology Parent Company of Changchun Institute of Applied Chemistry, and other chemicals involved were purchased from Beijing Chemical Company. All chemicals were of analytical grade and used directly without further purification.

A series of objective samples $Sr_2Y_8(SiO_4)_6O_2$ (SYSO) and $Sr_2Y_{8-x-y}(SiO_4)_6O_2:xBi^{3+}$, $yEu^{3+}$ were prepared by the Pechini-type sol-gel route.[13] The doping concentration of $Bi^{3+}$ and $Eu^{3+}$ are x = 0.01-0.40 and y = 0.04-0.56 in SYSO, respectively. First, $Y_2O_3$ and $Eu_2O_3$ were dissolved in dilute nitric acid ($HNO_3$) under constant stirring and heating to form a colorless solution of $Y(NO_3)_3$ and $Eu(NO_3)_3$, respectively. Stoichiometric amounts of $Y(NO_3)_3$, $Eu(NO_3)_3$, $Sr(NO_3)_2$ and $Bi(NO_3)_3{\cdot}5H_2O$ were dissolved in deionized water, with stirring for 10 min, after which the citric acid with the fixed stoichiometric value [2:1 (mol/mol) citric acid/metal ion] was added. Then, the pH of the solution was adjusted to ~2 with $HNO_3$ followed by the addition of a stoichiometric amount of tetraethyl orthosilicate [$Si(OC_2H_5)_4$] dissolved in ethanol after 20 min stirring. At last, a certain amount of poly(ethylene glycol) (PEG; molecular weight = 20000, analytical reagant grade) was appended as a cross-linking agent (CPEG = 0.005 mol/L) after stirring for about 15 min. The final mixtures were stirred for 2 h and then heated at 75 °C with a water bath to form homogeneous gels. Then, the obtained gels were prefired at 600 °C for 4 h in air followed by fully grinding and calcination at 1350 °C for 6h in a muffle furnace to generate the final powder materials.

### 2.2 Measurement and Characterization.

All the measurements were performed using the finely ground powder. D8 Focus diffractometer at a scanning rate of $10°min^{-1}$ in the 2θ range from 10° to 110° with graphite-monochromatized Cu $K_\alpha$ radiation (λ = 0.15405 nm) was used to check the phase purity of samples. Infrared spectra were obtained on a VERTEX 70 Fourier transform infrared (FT-IR) spectrometer (Bruker). The excitation source from a fluorescence spectrophotometer equipped with a 450 W xenon lamp (Edinburgh Instruments FLSP-920) was used to carry out the photoluminescence (PL) measurements. The luminescence decay lifetimes were measured and obtained from a Lecroy Wave Runner 6100 Digital Osilloscope (1 GHz) using a tunable laser (pulse width = 4 ns, gate = 50 ns) as the excitation (Contimuum Sunlite OPO) source. PL quantum yields (QYs) of as-prepared phosphors were obtained directly by the absolute PL QY measurement system (C9920-02, Hamamatsu Photonics K. K., Japan). All the measurements above were performed at room temperature (RT) condition. What's more, the temperature-dependent (298-523 K) PL spectra were measured on Edinburgh Instruments FLSP-920 with a temperature controller.

## 3. Results and Discussion

The phase composition and purity have been examined by GASA Rietveld refinements at room temperature for the representative SYSO:0.08$Bi^{3+}$ (Fig. 1a) and SYSO:0.08$Bi^{3+}$, 0.40$Eu^{3+}$ (Fig. 1b) samples. The original structure model and crystallographic data for the refinement were referred to $Sr_2Nd_8(SiO_4)_6O_2$ (ICSD 155627) compound. All the atomic positions, fraction factors, and thermal vibrational parameters were converged and refined. We can observe that the weighted profile R-factor ($R_{wp}$) and the expected R factor ($R_p$) are 5.67% and 3.81% for SYSO:0.08$Bi^{3+}$, and 6.77% and 4.12% for SYSO:0.08$Bi^{3+}$, 0.40$Eu^{3+}$ samples, respectively. This indicates the reflection conditions are well satisfied. Detailed information for the results is listed in Table 1. In addition, this result confirms that the structure of SYSO is isostructural with

View Article Online
DOI: 10.1039/C5TC01993A





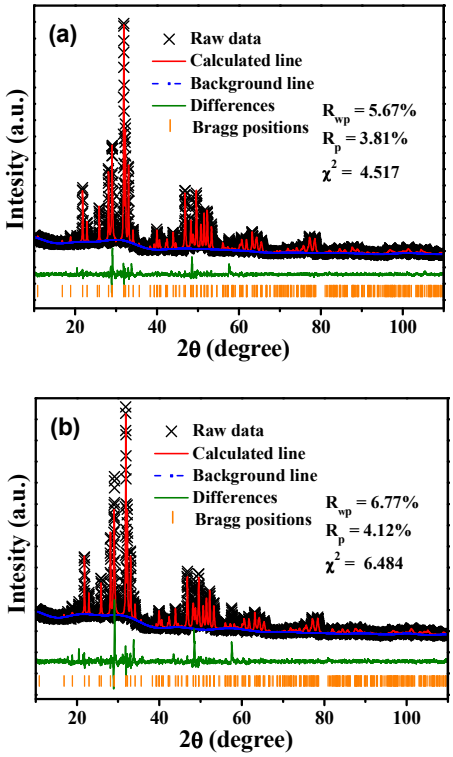


**Fig. 1** Rietveld refinements for SYSO:0.08$Bi^{3+}$ (a) and SYSO:0.08$Bi^{3+}$, 0.40$Eu^{3+}$ (b) samples.

$Sr_2Nd_8(SiO_4)_6O_2$. Therefore, SYSO crystallizes in hexagonal space group *P6₃/m* with two kinds of Y atom sites where *6h* site are completely occupied by Y1 with seven-fold coordination, while other Sr and Y are randomly distributed in *4f* site with nine-fold coordination, as depicted in Fig. 2a and b, respectively. The XRD patterns for as-prepared SYSO host and $Bi^{3+}$, $Eu^{3+}$-doped SYSO phosphors, as well as standard patterns of $Sr_2Nd_8(SiO_4)_6O_2$ (ICSD 155627) have been presented in Fig. 3. It is found that the diffraction positions of SYSO host and $Bi^{3+}$,

**Table 1** Crystallographic data and details in the data collection and refinement parameters for the SYSO:0.08$Bi^{3+}$ and SYSO:0.08$Bi^{3+}$, 0.40$Eu^{3+}$ samples.

| Sample | SYSO:0.08$Bi^{3+}$ | SYSO:0.08$Bi^{3+}$, 0.40$Eu^{3+}$ |
|---|---|---|
| Space group | *P6₃/m* | *P6₃/m* |
| Symmetry | hexagonal | hexagonal |
| a, Å | 9.3873(1) | 9.3976(2) |
| b, Å | 9.3873(1) | 9.3976(2) |
| c, Å | 6.8471 (2) | 6.8829 (2) |
| V, $Å^3$ | 524.60(2) | 526.42(0) |
| Z | 1 | 1 |
| 2θ-interval,° | 10-110 | 10-110 |
| $R_{wp}$ | 5.67 | 6.77 |
| $R_p$ | 3.81 | 4.12 |
| $\chi^2$ | 4.517 | 6.484 |

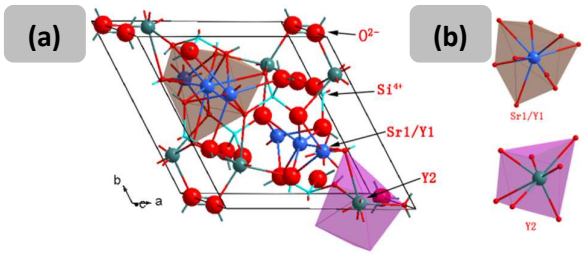


**Fig. 2** Crystal structure of SYSO (a) and coordination environment for Y1 and Y2 (b).

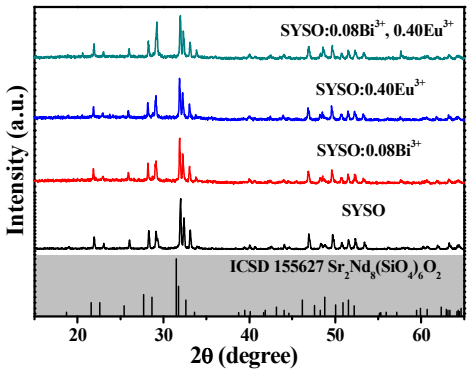


**Fig. 3** XRD patterns for SYSO host and SYSO: 0.08$Bi^{3+}$, SYSO: 0.40$Eu^{3+}$, and SYSO:0.08$Bi^{3+}$, 0.40$Eu^{3+}$ samples, as well as the standard pattern of $Sr_2Nd_8(SiO_4)_6O_2$ (ICSD 155627).

$Eu^{3+}$-doped SYSO phosphors shift to higher degree relative to $Sr_2Nd_8(SiO_4)_6O_2$ obviously. This is because the ionic radius of $Y^{3+}$ [0.96 Å for coordination number (CN=7) and 1.10 Å for CN=9] is smaller than that of $Nd^{3+}$ (1.06 Å for CN=7 and 1.19 Å for CN=9). However, their profiles are consistent with each other, indicating that all the patterns are well assigned to pure $Sr_2Y_8(SiO_4)O_2$ phase. The $Bi^{3+}$ and $Eu^{3+}$ are expected to substitute the Y sites based on their similar ionic radii ($Bi^{3+}$, 1.07 Å for CN=7 and 1.15 Å for CN=9, $Eu^{3+}$, 1.03 Å for CN=7 and 1.10 Å for CN=9) and same charge. Furthermore, the introductions of $Bi^{3+}$ and $Eu^{3+}$ ions into SYSO compound do not result in any other new phases.

The FT-IR spectra of the SYSO host and $Bi^{3+}$, $Eu^{3+}$-doped samples are presented in Fig. 4. We can observe that the profiles of FT-IR spectra of SYSO:0.08$Bi^{3+}$ and SYSO:0.08$Bi^{3+}$, 0.40$Eu^{3+}$ samples are similar to that of the SYSO host shown in Fig. 4a, indicating that the incorporations of $Bi^{3+}$ and $Eu^{3+}$ into this host have made little change to the structure of SYSO, consistent with the XRD analysis mentioned above. The two bond vibration positions around 513 and 559 $cm^{-1}$ correspond to the bending mode of the $SiO_4$ tetrahedron, and the peak around 931 $cm^{-1}$ is assigned to the asymmetric Si-O stretching modes of the $SiO_4$ tetrahedron. Those results are in good agreement with the data [400-600 $cm^{-1}$ refers to δ($SiO_4$) and 900-1100 $cm^{-1}$ refers to ν($SiO_4$)] reported in the previous paper.[14] Another three absorption peaks of FT-IR spectra at about 1630, 2924 and 3440 $cm^{-1}$ are attributed to the $OH^-$

View Article Online
DOI: 10.1039/C5TC01993A
ARTICLE Journal Name



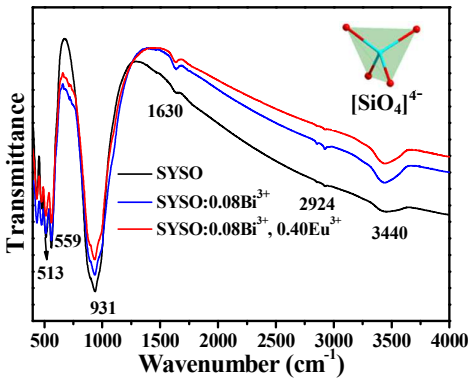


**Fig. 4** FT-IR spectra of as-prepared SYSO, SYSO:0.08$Bi^{3+}$ and SYSO:0.08$Bi^{3+}$, 0.40$Eu^{3+}$ samples.

stretching vibration mode arising from the covered water on the surface of samples under air condition.

Fig. 5a and b shows the PL excitation and emission spectra for SYSO:0.08$Bi^{3+}$ phosphor. The emission and absorption spectra are expected to present broad bands, which strongly depend on coordination number, covalence, bond volume polarizability and current charge, consistent with previously reported $Eu^{2+}$ and $Pb^{2+}$.[15] The ground state of $Bi^{3+}$ ions is $^1S_0$ with a $6s^2$ configuration, whereas the excited state is triplet state ($^3P_0$, $^3P_1$, $^3P_2$) originating from its 6s6p configuration and $^1P_1$ singlet state with rising excitation energy. Generally, the $^1S_0 \rightarrow {}^3P_0$ and $^1S_0 \rightarrow {}^3P_1$ absorption of $Bi^{3+}$ locates at ultraviolet area at room temperature. As depicted in Fig. 5a, the excitation spectrum detected at 493 nm displays a main band with the maximum at 331 nm and an unobvious one at 345 nm, originating from the $^1S_0 \rightarrow {}^3P_1$ transition of $Bi^{3+}$(2). Upon 345 nm excitation, the emission spectrum presents a broad wavelength range extending from 350 to 650 nm with two obvious emission bands around 413 and 493 nm, respectively. These two bands are ascribed to the $^3P_1 \rightarrow {}^1S_0$ transition of $Bi^{3+}$ in Fig. 5a. It is easily accepted that the two main emission peaks can be assigned to the occupations of two kinds of $Y^{3+}$ by $Bi^{3+}$. Based on the calculation of average bonds of Y-O,[16] the $Y^{3+}$(1)-O is much longer than that of $Y^{3+}$(2)-O, therefore, the coordinated bond of $Bi^{3+}$(1)-O is much weaker than that of $Bi^{3+}$(2)-O,[17]. Thus, we can infer that the band around 413 nm can be ascribed to the $^3P_1 \rightarrow {}^1S_0$ transition of $Bi^{3+}$ ions occupying the Y(1) sites with nine-coordination, denoted as $Bi^{3+}$(1), while the other one attributes to $Bi^{3+}$ ions replacing Y(2) ions with seven-coordination, denoted as $Bi^{3+}$(2). Fig. 5b illustrates the PL excitation spectrum monitored at 413 nm and emission spectrum excited into 373 nm. Only one band around at 413 nm from the emission spectrum can be observed. The emission position is consistent with that in Fig. 5a, therefore, this band is confirmed to be the $^3P_1 \rightarrow {}^1S_0$ transition of $Bi^{3+}$(1). The two primary bands around 340 and 373 nm can be assigned to the $^1S_0 \rightarrow {}^3P_0$ transition of $Bi^{3+}$(1). Moreover, we can observe that a minor excitation band around 260 nm occurs in both two excitations monitored at

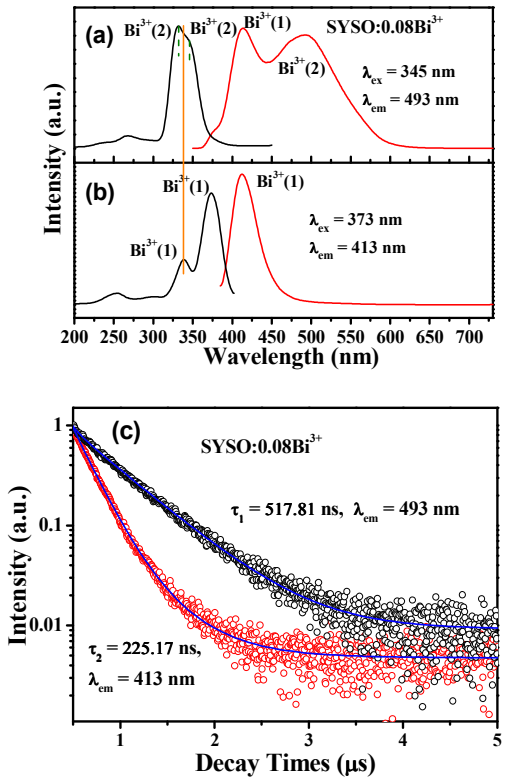


**Fig. 5** (a) PL excitation (monitored at 493 nm) and emission (excited at 345 nm) spectra for SYSO:0.08$Bi^{3+}$. (b) PL excitation (monitored at 413 nm) and emission (excited at 373 nm) spectra SYSO:0.08$Bi^{3+}$. (c) Fluorescent decay curves monitored at 413 and 493 nm with the excitation wavelength of 345 nm for SYSO:0.08$Bi^{3+}$.

413 and 493 nm and a minor emission around 375 nm, which may be attributed to the $Bi^{3+}$-$O^{2-}$ charge transfer transition. This is because the transition energy of charge transfer transition is higher than that of $^1P_1$-$^1S_0$ transition of $Bi^{3+}$.[18] Fig. 5c shows the fluorescence decay curves of $Bi^{3+}$ monitored at 413 [$Bi^{3+}$(1)] and 493 nm [$Bi^{3+}$(2)] with the excitation wavelength of 345 nm in SYSO:0.08$Bi^{3+}$, which can be well fitted with the double-order exponential decay, as expressed below:[19]

$$I(t) = A_1 \exp(-t/\tau_1) + A_2 \exp(-t/\tau_2) + I_0 \quad (1)$$

where $I$(t) is the luminescence intensity at certain time t, $A_1$ and $A_2$ are constants, $\tau_1$ and $\tau_2$ are rapid and slow times for the exponential components, respectively. The effective decay times can be approximately calculated as follow:

$$\tau^* = \left(A_1\tau_1^2 + A_2\tau_2^2\right) / \left(A_1\tau_1 + A_2\tau_2\right) \quad (2)$$

According to the equation above, we can calculate that the decay times at 413 nm and 493 nm are 225.17 ns and 517.81 ns, respectively. It is evident that they are very different from each other. This result validates that two kinds of $Bi^{3+}$ emission bands exist in SYSO:0.08$Bi^{3+}$ phosphor.

View Article Online
DOI: 10.1039/C5TC01993A




Fig. 6 shows the PL emission spectra of SYSO:xBi$^{3+}$ upon 340 nm excitation with different concentrations of Bi$^{3+}$. It is observed that the profiles of emission spectra are similar to each other. The emission intensity first increases with the increase of Bi$^{3+}$ concentration until the maximum x = 0.08, after which the intensity begins to decrease monotonously with further increasing Bi$^{3+}$ concentration attributed to the concentration quenching effect, as illustrated in Fig. 6. It is accepted that concentration quenching effect takes place due to the energy transfer between Bi$^{3+}$ ions, whose probability raises as the concentration of Bi$^{3+}$ increases. In order to approximately assess the energy transfer mechanism between Bi$^{3+}$, it is necessary to know the critical distance ($R_c$) between activators such as Bi$^{3+}$. The distance between Bi$^{3+}$ becomes shorter and shorter with increasing Bi$^{3+}$ content, leading to the increase of energy transfer probability. When the distance is small enough, the concentration quenching happens and the energy migration is blocked. The $R_c$ can be calculated using the concentration quenching method as given by the expression:[20]

$$R_c \approx 2\left[\frac{3V}{4\pi X_c N}\right]^{1/3} \quad (3)$$

where $V$ and $N$ correspond to the volume of the unit cell and the number of available sites for the dopant in the unit cell, respectively, and $X_c$ is the critical concentration of dopant ions. For the SYSO host, $N$ = 1, $V$ = 524.076 Å$^3$,[16] and $X_c$ is 0.08 for Bi$^{3+}$; Consequently, the critical distance ($R_c$) was determined to be about 23.21 Å.

Since the exchange interaction generally occurs in the forbidden transition whose $R_c$ is typically 5Å, therefore, the result above is much bigger than it, indicating little possibility of this mechanism. The mechanism of radiation reabsorption is only efficacious which requires the wide overlap between fluorescence and absorption spectra. We can find this is also not considered to take place here. As a result, it can be inferred that the electric multipole interaction contributes to the non-radiative concentration quenching between two nearest Bi$^{3+}$ centers based on the Dexter theory:[21]

$$\frac{I}{x} = \left[1+\beta\left(x\right)^{\theta/3}\right]^{-1} \quad (4)$$

where $I$ refers to the emission intensity, $x$ is Bi$^{3+}$ concentration beyond the optimal value, and $\theta$ represents a constant for the given matrix under the identical excitation conditions. The type of energy transfer mechanism of electric multipole interaction can be determined by analyzing the constant $\vartheta$ from this formula, in which the value of $\vartheta$ = 6, 8, and 10 correspond to dipole–dipole, dipole–quadrupole, and quadrupole–quadrupole interactions, respectively. Fig. 7 illustrates the dependences of I/x on x on a logarithmic scale for two kinds of Bi$^{3+}$. The two approximately fitting linear relations between log(I/x) and log(x) for Bi$^{3+}$(1) and Bi$^{3+}$(2) are also given. The slopes of fitted straight lines are equal to -1.98 and -1.94 = -$\vartheta$/3 for Bi$^{3+}$(1) and Bi$^{3+}$(2), respectively. As a consequence, the $\vartheta$ = 5.94 and 5.82 are approximately both as

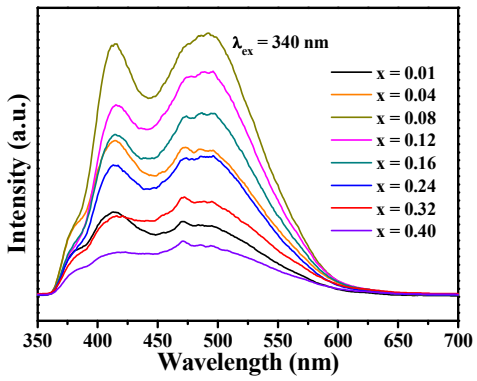


**Fig. 6** PL emission spectra of SYSO:xBi$^{3+}$ (x = 0.01-0.40) upon 340 nm excitation.

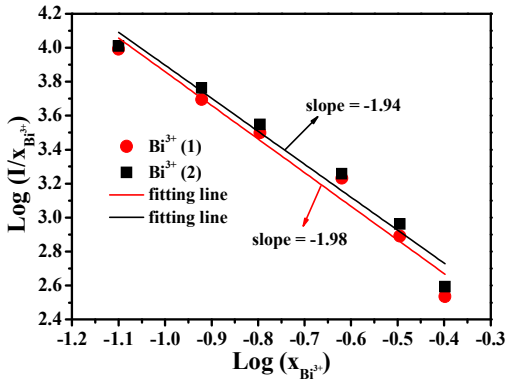


**Fig. 7** Linear fitting of log(x) versus log(I/x) in various SYSO: xBi$^{3+}$ phosphors with two kinds of Bi$^{3+}$ beyond the concentration quenching (x > 0.08).

6, indicating the dipole-dipole interactions are responsible for the energy transfer between Bi$^{3+}$ in SYSO:Bi$^{3+}$ phosphors.

The PL properties of SYSO:0.40Eu$^{3+}$ sample are shown in Fig. 8a. The PL excitation spectrum monitored at 615 nm shows one wide excitation band from 200 to 350 nm centered at 272 nm and several sharp lines peaking at 363, 383, 396, 466 and 534 nm from 350 to 550 nm, which can be assigned to the charge transfer (CT) transition of Eu$^{3+}$-O$^{2-}$ and $^7F_0 \rightarrow {}^5D_4$, $^7F_0 \rightarrow {}^5L_7$, $^7F_0 \rightarrow {}^5L_6$, $^7F_0 \rightarrow {}^5D_2$, and $^7F_0 \rightarrow {}^5D_1$ transitions of Eu$^{3+}$, respectively.[22] The emission position of CT band varies relying on the different hosts. The PL emission spectra under 272 and 466 nm excitation are similar to each other, and they both include many emission lines in the region from 550 nm to 750 nm, which are assigned to the transitions of $^5D_0 \rightarrow {}^7F_J$ ( J = 0, 1, 2, 3, 4) of Eu$^{3+}$. The peak at 538 nm is ascribed to the transition of $^5D_1 \rightarrow {}^7F_1$ of Eu$^{3+}$ ion. The peaks at 589 and 595 nm originate from the $^5D_0 \rightarrow {}^7F_1$ magnetic-dipole transition. This transition is considered to be insensitive to site symmetry. The red emission $^5D_0 \rightarrow {}^7F_2$ electric-dipole transition is produced due to the lack of inversion symmetry at the Eu$^{3+}$ site and can be much stronger than that to the $^7F_1$ level. When the Eu$^{3+}$ ions locate at low local symmetry environment, the hypersensitive transition of $^5D_0$-$^7F_2$ dominates their emission spectrum. Based on the valence state and the ionic radius, the doped Eu$^{3+}$ ions

View Article Online
DOI: 10.1039/C5TC01993A




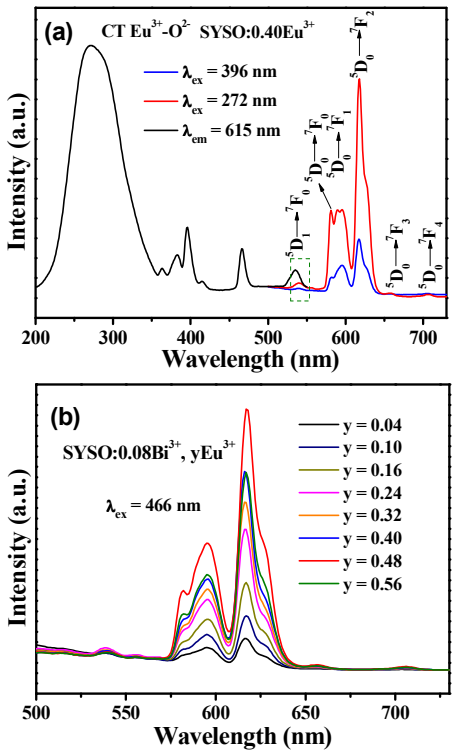


**Fig. 8** (a) PL ($\lambda_{ex}$ = 272 nm) and PLE ($\lambda_{em}$ = 615 nm) spectra of SYSO:0.40Eu$^{3+}$ sample. (b) PL emission spectra for SYSO:0.08Bi$^{3+}$, yEu$^{3+}$ (y = 0.04, 0.10, 0.16, 0.24, 0.32, 0.40, 0.48 and 0.56) in Eu$^{3+}$ doped concentration ($\lambda_{ex}$ = 466 nm).

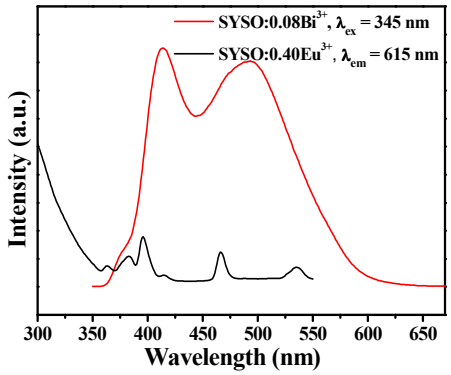


**Fig. 9** Spectral overlap of Eu$^{3+}$ excitation spectrum monitored at 615 nm in SYSO:0.40Eu$^{3+}$ and emission spectrum excited at 345 nm in SYSO:0.08Bi$^{3+}$.

are apt to occupy the Y$^{3+}$ sites in SYSO, making the $^5D_0$-$^7F_2$ emission of Eu$^{3+}$ at 615 nm be the prominent peak in the emission spectrum. The ratio of I($^5D_0$→$^7F_1$)/I($^5D_0$→$^7F_2$) strongly depends on the local symmetry of Eu$^{3+}$ ions in the host.[23] In this case, the $^5D_0$→$^7F_2$ transition at 615 nm becomes the dominant one, indicating that Eu$^{3+}$ ions occupy the site without inversion symmetry. The PL emission spectra of SYSO:0.08Bi$^{3+}$, yEu$^{3+}$ (y = 0.04, 0.10, 0.16, 0.24, 0.32, 0.40, 0.48 and 0.56) with different Eu$^{3+}$ concentrations ($\lambda_{ex}$ = 466 nm) are shown in Fig. 8b. The characteristic emission of Eu$^{3+}$ ion here indicates that

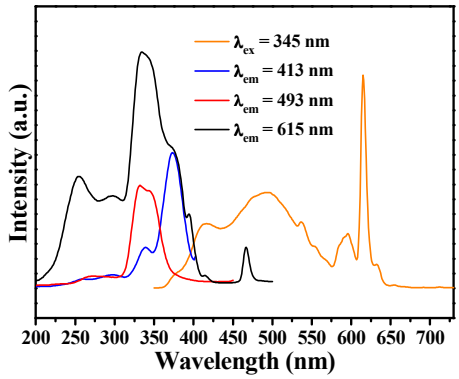


**Fig. 10** PL excitation spectra monitored at 413, 493 and 615 nm, and emission spectrum upon 345 nm excitation in SYSO:0.08Bi$^{3+}$, 0.40Eu$^{3+}$.

the phosphors also can be utilized as red phosphors with a blue chip.

In order to explore the possibility of energy transfer from Bi$^{3+}$ to Eu$^{3+}$ ions, the excitation spectrum monitored at 615 nm in SYSO:0.40Eu$^{3+}$ and emission spectrum excited at 345 nm in SYSO:0.08Bi$^{3+}$ were detected and supplied in Fig. 9. A significant spectral overlap can be easily observed. This result gives the probable energy transfer from Bi$^{3+}$ to Eu$^{3+}$ ions when they are co-doped into SYSO host. The energy transfer mechanism from Bi$^{3+}$ to Eu$^{3+}$ ions was expected to be the resonance type according to the proposal from Dexter's.[24] In addition, the existence of energy transfer can be demonstrated by the PL emission and excitation spectra in SYSO:0.08Bi$^{3+}$, 0.40Eu$^{3+}$ sample, as illustrated in Fig. 10. Upon 345 nm excitation, the emission spectrum exhibits not only blue-green area from Bi$^{3+}$ but also some sharp red component from Eu$^{3+}$. The excitation spectra monitored at 413 and 493 nm are well consistent with those obtained in Bi$^{3+}$ single doped SYSO sample in Fig. 5. This demonstrates that the blue-green band in emission spectrum is originated from Bi$^{3+}$. Monitored at 615 nm of Eu$^{3+}$ transition, the excitation spectrum consists of O$^{2-}$-Eu$^{3+}$ charge transfer band, characteristic Eu$^{3+}$ excitation lines, and the obvious 331 and 345, and 373 nm bands from Bi$^{3+}$, confirming the energy transfer from Bi$^{3+}$(1) and Bi$^{3+}$(2) to

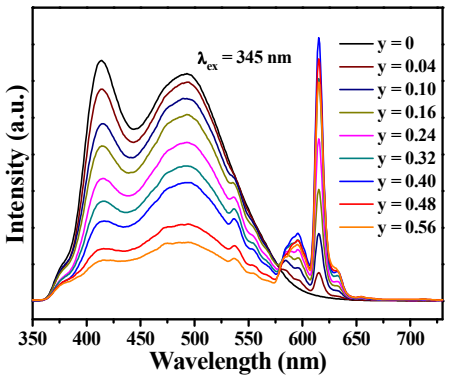


**Fig. 11** PL emission spectra for SYSO:0.08Bi$^{3+}$, yEu$^{3+}$ (y = 0, 0.04, 0.10, 0.16, 0.24, 0.32, 0.40, 0.48 and 0.56) excited at 345 nm.

View Article Online
DOI: 10.1039/C5TC01993A




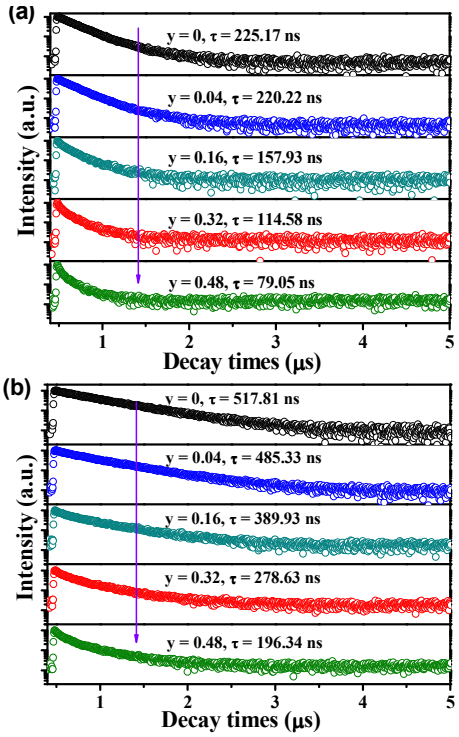


**Fig. 12** Fluorescent decay curves for $Bi^{3+}$(1) at 413 nm (a) and $Bi^{3+}$(2) at 493 nm (b) upon 345 nm excitation with increasing $Bi^{3+}$ concentration in SYSO:0.08$Bi^{3+}$, y$Eu^{3+}$.

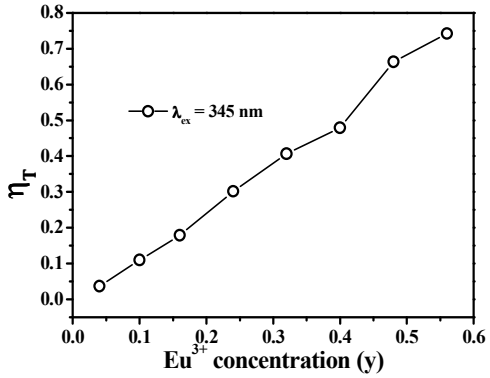


**Fig. 13** Energy transfer efficiency ($\eta_T$) in SYSO:0.08$Bi^{3+}$, y$Eu^{3+}$ phosphors with different $Eu^{3+}$ concentrations.

$Eu^{3+}$. Additionally, we can observe that the excitation intensities at 331, 345 nm and 373 nm are all stronger than that of $Eu^{3+}$-$O^{2-}$ charge transfer band around 272 nm, which is highly expected in $Eu^{3+}$ doped phosphors. The PL excitation spectrum of $Eu^{3+}$, $Bi^{3+}$ co-doped SYSO phosphor matches well with the UV chip, as observed from Fig. 10, indicating that this phosphor can be potentially applied for UV-chip w-LEDs.

To further study the energy transfer properties from $Bi^{3+}$ to $Eu^{3+}$ ions, a series of $Bi^{3+}$, $Eu^{3+}$ co-doped SYSO samples were synthesized. Fig. 11 shows the variation of PL emission spectra as a function of $Eu^{3+}$ concentration in SYSO:0.08$Bi^{3+}$, y$Eu^{3+}$ samples. We can find the emission intensity of $Bi^{3+}$ presents a monotonous decrease with gradually increasing $Eu^{3+}$

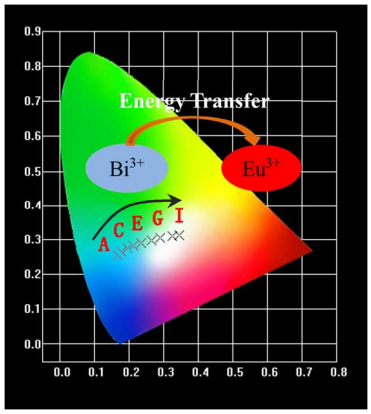


**Fig. 14** CIE chromaticity diagram for SYSO: 0.08$Bi^{3+}$, y$Eu^{3+}$ samples (y = 0, 0.04, 0.10, 0.16, 0.24, 0.32, 0.40, 0.48 and 0.56).

concentration with the excitation wavelength of 345 nm. The PL emission intensity of red component increases until the maximum y = 0.40 with increasing $Eu^{3+}$ ion concentration. The subsequent decrease of $Eu^{3+}$ emission intensity beyond y = 0.40 takes place because of the general concentration quenching effect. This result gives us a further confirmation of existent energy transfer from $Bi^{3+}$ to $Eu^{3+}$ ions in SYSO:$Bi^{3+}$, $Eu^{3+}$. To support the spectra analysis, the fluorescent decay curves located at $Bi^{3+}$(1) and $Bi^{3+}$(2) emission bands were measured with the excitation wavelength of 345 nm and plotted in Fig. 12, which can be fitted with the second-order exponential decay given above. The values of decay times are determined to be 225.17, 220.22, 157.93, 114.58 and 79.05 ns for $Bi^{3+}$(1) at 413 nm, and 517.81, 485.33, 389.93, 278.63 and 196.34 ns for $Bi^{3+}$(2) at 493 nm corresponding to the y = 0, 0.04, 0.16, 0.32 and 0.48, respectively, indicating the monotonous decrease of decay times with increasing $Eu^{3+}$ concentration in SYSO:0.08$Bi^{3+}$, y$Eu^{3+}$ samples. The result can strongly prove the existence of energy transfer from $Bi^{3+}$ to $Eu^{3+}$ ions.

Moreover, in view of this host, the energy transfer efficiency ($\eta_T$) from sensitizer $Bi^{3+}$ to acceptors $Eu^{3+}$ can be approximately estimated using following equation:[25]

$$\eta_T = 1 - \frac{I_S}{I_{S0}} \quad (5)$$

where $\eta_T$ represents the value of energy transfer efficiency, $I_{S0}$ and $I_S$ are the luminescence intensities of $Bi^{3+}$ ions without and with the existence of $Eu^{3+}$ ions, respectively. Fig. 13 plots the curve of calculated value of $\eta_T$ from $Bi^{3+}$ to $Eu^{3+}$ in SYSO:0.08$Bi^{3+}$, y$Eu^{3+}$ samples under 345 nm excitation as a function of $Eu^{3+}$ concentration. The calculated $\eta_T$ value rises monotonously with increasing $Eu^{3+}$ concentration in this concentration interval, which can reach the maximum of 74%. Therefore, the energy transfer from $Bi^{3+}$ to $Eu^{3+}$ ions is reckoned to be an efficient process in SYSO:$Bi^{3+}$, $Eu^{3+}$ phosphors.

The CIE chromaticity diagram for SYSO:0.08$Bi^{3+}$, y$Eu^{3+}$ samples (y = 0, 0.04, 0.10, 0.16, 0.24, 0.32, 0.40, 0.48 and 0.56) is displayed in Fig. 14 with the corresponding value of

View Article Online
DOI: 10.1039/C5TC01993A




**Table 2** The variation of CIE chromaticity coordinates (x, y) and QYs for SYSO:0.08$Bi^{3+}$, y$Eu^{3+}$ phosphors excited at 345 nm.

| Sample no. | $Eu^{3+}$ concentration (y mol) | CIE coordinates (x, y) | QY (%) |
|---|---|---|---|
| A | 0 | (0.168, 0.255) | 74.8 |
| B | 0.04 | (0.177, 0.264) | 48.9 |
| C | 0.10 | (0.194, 0.274) | 40.2 |
| D | 0.16 | (0.212, 0.282) | 44.1 |
| E | 0.24 | (0.236, 0.291) | 49.0 |
| F | 0.32 | (0.265, 0.298) | 61.3 |
| G | 0.40 | (0.290, 0.305) | 69.0 |
| H | 0.48 | (0.325, 0.311) | 52.0 |
| I | 0.56 | (0.347, 0.312) | 33.9 |

calculated CIE chromaticity coordinates (x, y) in Table 2. With increasing $Eu^{3+}$ concentration in SYSO:0.08$Bi^{3+}$, y$Eu^{3+}$ samples, the CIE chromaticity coordinate varies from (0.168, 0.255) to (0.347, 0.312) corresponding to y = 0 and 0.56, located at blue-green and white areas, respectively. Therefore, the emission color can be tuned from blue-green to white in SYSO:$Bi^{3+}$, $Eu^{3+}$ by adjusting the concentrations of $Bi^{3+}$ and $Eu^{3+}$ ions. The obtained quantum yield (QYs) of SYSO:0.08$Bi^{3+}$ is 74.8%, and the maximum can reach 69.0% for SYSO:0.08$Bi^{3+}$, 0.40$Eu^{3+}$ sample in $Bi^{3+}$, $Eu^{3+}$ co-doped SYSO samples, as listed in Table 2.

As presented above, for this host, the $R_c$ is determined to be 12.78 Å by utilizing the equation (2), in which the different $X_c$ value is denoted as the critical concentration of dopant ions (total concentration of $Bi^{3+}$ and $Eu^{3+}$, approximately 0.48), that is, at which the luminescence intensity of $Bi^{3+}$ is half of that in the sample without the existence of $Eu^{3+}$. The result also excludes the mechanisms of exchange interaction and radiation reabsorption based on analysis, indicating the electric multipole interaction would be responsible for energy transfer from $Bi^{3+}$ to $Eu^{3+}$ ions in SYSO:$Bi^{3+}$, $Eu^{3+}$. According to the Dexter's energy transfer formula of multipolar interaction, the following relationship can be adopted:[26]

$$\frac{\eta_{S0}}{\eta_S} \propto C^{\alpha/3} \quad (6)$$

where $\eta_{S0}$ and $\eta_S$ stand for the luminescence quantum efficiencies of the $Bi^{3+}$ ions with the absence and presence of the $Eu^{3+}$ ions, respectively. $C$ represents the total values of the $Bi^{3+}$ and $Eu^{3+}$ ions concentrations. The values $\alpha$ = 6, 8 and 10 correspond to dipole-dipole, dipole-quadrupole, and quadrupole-quadrupole interactions, respectively. However, the $\eta_{S0}/\eta_S$ is difficult to be determined and therefore it can be assessed instead by the $I_{S0}/I_S$, where $I_{S0}$ and $I_S$ stand for the luminescence intensities of $Bi^{3+}$ ions without and with the existence of $Eu^{3+}$ ions, respectively, accordingly, the above equation can be replaced as follows:

$$\frac{I_{S0}}{I_S} \propto C^{\alpha/3} \quad (7)$$

The relationship between $I_{S0}/I_S$ and $C^{\alpha/3}$ based on the above equation are plotted in Fig. 15. One can find that the value of $R^2$ with the linear fitting in Fig. 15b is bigger than those in Fig.

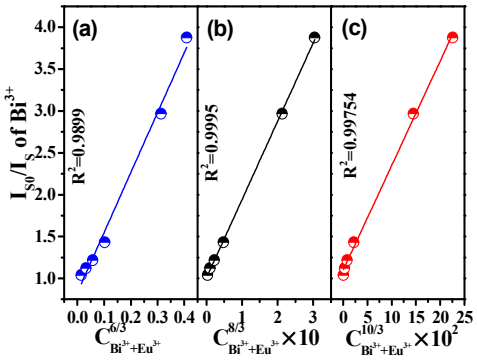


**Fig. 15** Dependence of ($I_{S0}/I_S$) of $Bi^{3+}$ on (a) $C^{6/3}$ (b) $C^{8/3}$ and (c) $C^{10/3}$.

15a and c, indicating that the best linear behavior occurs when α = 8. Consequently, the dipole-quadrupole mechanism contributes to the energy transfer process from $Bi^{3+}$ to $Eu^{3+}$ ions.

In view of the dipole-quadrupole interaction, the $R_c$ value also can be obtained through the spectral overlap route which has the formula displayed as follows:[27]

$$R_c^8 = 3.024\times10^{12}\lambda_S^2 f_q \int f_S(E) f_A(E)/E^4 dE \quad (8)$$

In our case, it is a pity that $f_q$ of $Eu^{3+}$ has not been obtained so far. However, Verstegen et al. proposed that $f_q/f_d$ = $10^{-3}$-$10^{-2}$ can be reasonable, $f_d$ = $10^{-6}$ is the oscillator strength of the electric dipole transitions.[28] $\lambda_S$ (4130 Å) and E are the wavelength of strongest intensity of $Bi^{3+}$ and the energy involved in the transfer (in eV); $\int f_S(E)f_A(E)/E^4$ dE stands for the spectral overlap between the normalized shapes of the sensitizer $Bi^{3+}$ emission $f_S(E)$ and the activator $Eu^{3+}$ excitation $f_A(E)$, and in this condition it is determined to be about 0.00198 $eV^{-5}$. As a result, the value of $R_c$ is calculated to be 10.03-13.37 Å, which agrees well with that calculated by concentration quenching method above (12.78 Å). This result can further testify that the electric dipole-quadrupole interaction would be responsible for the energy transfer mechanism from $Bi^{3+}$ to $Eu^{3+}$ ions in SYSO:$Bi^{3+}$, $Eu^{3+}$ samples.

As an important parameter for LED fabrication and application, thermal quenching properties of representative of SYSO: 0.08$Bi^{3+}$, 0.40$Eu^{3+}$ sample has been investigated with the temperature range of 298-523 K. The measured variations of emission spectra and emission intensity of $Bi^{3+}$ and $Eu^{3+}$ have been plotted in Fig. 16a. We can observe the emission intensity decreases monotonously with increasing operated temperature. It is accepted that the reason for the decrease of emission intensity is attributed to the thermal quenching via the thermal activation through the crossing point between the ground and the excited states. At 150 ℃, the emission intensity of $Bi^{3+}$ and $Eu^{3+}$ keep about 65% and 41% of their corresponding initial values, respectively. It is clear the declined rate is different for $Bi^{3+}$ and $Eu^{3+}$ ions in SYSO: 0.08$Bi^{3+}$, 0.40$Eu^{3+}$. The reason for this is that the energy transfer process from $Bi^{3+}$ to $Eu^{3+}$ ions is also affected by the temperature. Moreover, the light blue-shift of $Bi^{3+}$ emission

View Article Online
DOI: 10.1039/C5TC01993A




position also can be found, which is common in many phosphors.[29] In order to better understand the quenching phenomenon, the Arrhenius formula concerning the relationship between temperature and luminescence intensity was used, which can be copied as follow:[30]

$$In\left(\frac{I_0}{I}\right) = InA - \frac{E_a}{kT} \qquad (9)$$

where $E_a$ is the objective activation energy, $A$ is a constant, $T$ represents the temperature (K) and $k$ is the Boltzmann constant ($8.626\times10^{-5}$ eV). $I_0$ and $I$ are the integrated intensity at the room emission intensity and differently operated temperatures, respectively. Therefore, we plot the relationship of $In(I_0/I\text{-}1)$ versus 1/kT activation energy graph for thermal quenching of SYSO: $0.08Bi^{3+}$, $0.40Eu^{3+}$ phosphor in Fig. 16b. The slope of fitting line is -0.2283, therefore, the activation energy $E_a$ can be inferred to be approximate 0.2283 eV. The relative high value indicates its good thermal property.

## Conclusions

A series of $Bi^{3+}$, $Eu^{3+}$ -doped SYSO phosphors were synthesized by Pechini-type sol–gel route. $Bi^{3+}$ singly -doped SYSO presents intense blue-green emission with the wavelength ranging from 350-650 nm under UV excitation. When $Eu^{3+}$ and $Bi^{3+}$ were co-doped into the SYSO, the efficient energy transfer from $Bi^{3+}$ to $Eu^{3+}$ may occur, which is deduced by the spectral overlap between $Bi^{3+}$ emission and $Eu^{3+}$ excitation in $Bi^{3+}$ and $Eu^{3+}$ singly doped SYSO, and demonstrated by the PL emission spectra under UV excitation and excitation spectra monitored at $Bi^{3+}$ and $Eu^{3+}$ emissions, as well as the decay times of $Bi^{3+}$ emission bands in SYSO:$Bi^{3+}$, $Eu^{3+}$ phosphors. The non-radiate energy transfer mechanism is determined to be dipole-quadrupole interaction, which is further illustrated via the consistence of calculated critical distances of energy transfer from $Bi^{3+}$ to $Eu^{3+}$ ions by concentration quenching (12.78 Å) and spectral overlap methods (10.03-13.37 Å). The emission color of SYSO: $Bi^{3+}$, $Eu^{3+}$phosphor can be tuned from blue-green area (0.168, 0.255) to white region (0.347, 0.312) in our experimental data by adjusting the concentrations of $Bi^{3+}$ and $Eu^{3+}$, white emission is realized for SYSO:$0.08Bi^{3+}$, $0.48Eu^{3+}$ with the CIE chromaticity coordinate (0.325, 0.311). The maximum value of quantum yield is determined to be 69% for SYSO:$0.08Bi^{3+}$, $0.40Eu^{3+}$ in $Bi^{3+}$, $Eu^{3+}$ co-doped SYSO samples. Moreover, the SYSO:$0.08Bi^{3+}$, $0.40Eu^{3+}$ shows good thermal quenching properties. The results above indicate that SYSO:$Bi^{3+}$, $Eu^{3+}$ phosphor possesses the potential as a single-component tunable emission (including white) phosphor for UV w-LEDs.

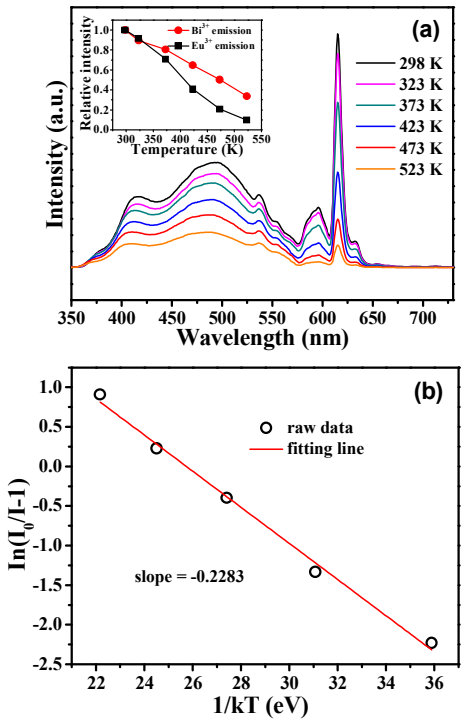


**Fig. 16** (a) Emission spectra of SYSO:$0.08Bi^{3+}$, $0.40Eu^{3+}$ as a function of temperature, inset is the variation of emission intensity of $Bi^{3+}$ and $Eu^{3+}$. (b) Linear fitting of $In(I_0/I\text{-}1)$ versus 1/kT activation energy graph for thermal quenching for SYSO: $0.08Bi^{3+}$,$0.40Eu^{3+}$ sample.

## Acknowledgements

This project is financially supported by the Scientific and Technological Department of Jilin Province (Grant No. 20150520029JH), National Natural Science Foundation of China (NSFC Grants 51472234, 51172227, 91433110), National Basic Research Program of China (Grants 2014CB643803), and Joint Funds of the National Natural Science Foundation of China (Grant U1301242).

## References

1 (a) T. Nishida,T. Ban and N. Kobayashi, *Appl. Phys. Lett*., 2003, **82**, 3817; (b) K. Li, J. Xu, X. Cai, J. Fan, Y. Zhang, M. Shang, H. Lian and J. Lin, *J. Mater. Chem. C*, 2015, **3**, 6341; (c) J. H. Oh, S. J. Yang and Y. R. Do, *Light*:*Sci. & Appl*., 2014, **3**, e141; (d) C.-H. Huang, T.-S. Chan, W.-R. Liu, D.-Y. Wang, Y.-C. Chiu, Y.-T. Yeh and T.-M. Chen, *J. Mater. Chem*., 2012, **22**, 20210; (e) S.-P. Lee, T.-S. Chan and T.-M. Chen, *ACS Appl. Mater. Interfaces*, 2015, **7**, 40; (f) H. Zhu, C. C. Lin, W. Luo, S. Shu, Z. Liu, Y. Liu, J. Kong, E. Ma, Y. Cao, R.-S. Liu and X. Chen, *Nat. Commun*., 2014, **5**, 4312; (g) Y. H. Liu, J. H. Hao, W. D. Zhuang, and Y. S. Hu, *J. Phys. D: Appl. Phys*., 2009, **42**, 245102; (h) Q. Zhang, J. Wang, G. Zhang and Q. Su, *J. Mater. Chem.*, 2009, **19**, 7088.

2 (a) Q. Xu,L. Han,Q. Di and J. Sun, *Ceram. Inter*., 2015, **41**, 2699; (b) V. Bachmann, C. Ronda and A. Meijerink, *Chem. Mater*., 2009, **21**, 2077; (c) C. Liang, H. You, Y. Fu, X. Teng, K. Liu and J. He, *Dalton Trans*., 2015, **44**, 8100.

3 (a) Z. Lian, J. Sun, L. Zhang, D. Shen, G. Shen, X. Wang and Q. Yan, *RSC Adv*., 2013, **3**, 16534; (b) F. Xiao, Y. N. Xue and Q. Y. Zhang, *Spectrochimica Acta Part A*, 2009, **74**, 498; (c) G. Zhu, S. Xin, Y. Wen, Q. Wang, M. Que and Y. Wang, *RSC Adv*., 2013, **3**, 9311.

View Article Online
DOI: 10.1039/C5TC01993A


4 (a) W. Tang and Z. Zhang, *J. Mater. Chem. C*, 2015, **3**, 5339; (b) W.-R. Liu and P.-C. Lin, *Opt. Exp.*, 2014, **22**, A446; (c) Y. Liu, X. Zhang, Z. Hao, X. Wang and J. Zhang, *Chem. Commun.*, 2011, **47**, 10677; (d) W. Lv, Z. Hao, X. Zhang, Y. Luo, X. Wang and J. Zhang, *Inorg. Chem.*, 2011, **50**, 7846; (e) Y. Zhang, D. Geng, M. Shang, Y. Wu, X. Li, H. Lian, Z. Cheng and J. Lin, *Eur. J. Inorg. Chem.*, 2013, **25**, 4389; (f) K. Li, D. Chen, R. Zhang, Y. Yu, J. Xu and Y. Wang, *Mater. Res. Bull.*, 2013, **48**, 1957.
5 (a) P. Dai, X. Zhang, L. Bian, S. Lu, Y. Liu and X. Wang, *J. Mater. Chem. C*, 2013, **1**, 4570; (b) W.-R. Liu, C.-H. Huang, C.-W. Yeh, J.-C. Tsai, Y.-C. Chiu, Y.-T.Yeh and R-S. Liu, *Inorg. Chem.*, 2012, **51**, 9636; (c) D. Geng, M. Shang, Y. Zhang, H. Lian, Z. Cheng and J. Lin, *J. Mater. Chem. C*, 2013, **1**, 2345.
6 (a) S. Yan, J. Zhang, X. Zhang, S. Lu, X. Ren, Z. Nie and X. Wang, *J. Phys. Chem. C*, 2007, **111**, 13256; (b) G. Dong, C. Hou, Z. Yang, P. Liu, C. Wang, F. Lu and X. Li, *Ceram. Inter.*, 2014, **40**, 14787; (c) L. Wan, S. Lü, L. Sun and X. Qu, *Opt. Mater.*, 2014, **36**, 628; (d) P. H. Yang, X. Yu, H. L. Yu, T. M. Jiang, X. H. Xu, Z. W. Yang, D. C. Zhou, Z. G. Song, Y. Yang, Z. Y. Zhao and J. B. Qiu, *J. Lumin.*, 2013, **135**, 206.
7 (a) J. Wang, Y. Huang, X. Wang, L. Qin and H. J. Seo, *Mater. Res. Bull.*, 2014, **55**, 126; (b) W. Lv, Y. Jia, Q. Zhao, M. Jiao, B. Shao , W. Lü and H. You, *RSC Adv.*, 2014, **4**, 7588.
8 (a) G. Li, D. Deng, X. Su, Q. Wang, Y. Li, Y. Hua, L. Huang, S. Zhao, H. Wang, C. Li and S. Xu, *Mater. Lett.*, 2011, **65**, 2019; (b) G. Li, Y. Zhang, D. Geng, M. Shang, C. Peng, Z. Cheng and J. Lin, *ACS Appl. Mater. Interface*, 2012, **4**, 296; (c) G. Li, D. Geng, M. Shang, C. Peng, Z. Cheng and J. Lin, *J. Mater. Chem.*, 2011, **21**, 13334; (d) X. Han, J. Lin, Z. Li, X. Qi, M. Li and X. Wang, *J. Rare Earths*, 2008, **26**, 443; (e) Y. Wen, Y. Wang, F. Zhang and B. Liu, *Mater. Chem. Phys.*, 2011, **129**, 1171.
9 (a) X. M. Han, J. Lin, H. L. Zhou, M. Yu, Y. H. Zhou and M. L. Pang, *J. Phys.*: *Condens. Matter*, 2004, **16**, 2745; (b) Y. Wen, Y. Wang, B. Liu and F. Zhang, *Opt. Mater.*, 2012, **34**, 889.
10 H. Zhou, Y. Jin, M. Jiang, Q. Wang and X. Jiang, *Dalton Trans.*, 2015, **44**, 1102.
11 Y. Shen, R. Chen, F. Xiao, H. Sun, A. Tok and Z. Dong, *J. Solid State Chem.*, 2010, **183**, 3093.
12 J. Sokolnicki and E. Zych, *J. Lumin.*, 2015, **158**, 65.
13 J. Lin, M. Yu, C. Lin and X. Liu, *J. Phys. Chem. C*, 2007, **111**, 5835.
14 (a) G. Buhler, A. Zharkouskaya and C. Feldmann, *Solid State Sci.*, 2008, **10**, 461; (b) D. V. Sunitha, H. Nagabhushana, F. Singh, S. C. Sharma, N. Dhananjaya, B. M. Nagabhushana and R. P. S. Chakradhare, *Spectrochim. Acta, Part A*, 2012, **90**, 18.
15 (a) L. G. Jacobsohn, M. W. Blair, S. C. Tornga, L. O. Brown, B. L. Bennett and R. E. Muenchausen, *J. Appl. Phys.*, 2008, **104**, 124303; (b) L. Wang, Q. Sun, Q. Liu and J. Shi, *J. Solid State Chem.*, 2012, **191**, 142.
16 Y. Shen, A. Tok and Z. Dong, *J. Am. Ceram. Soc.*, 2010, **93**, 1176.
17 H. Ju, W. Deng, B. Wang, J. Liu, X. Tao and S. Xu, *J. Alloys Compd.*, 2012, **516**, 153.
18 K. P. Oboth, F. J. Lohmeier and F. Fischer, *Phys. Status Solidi B*, 1989, **154**, 789.
19 (a) Z. Yang, P. Liu, L. Lv, Y. Zhao, Q. Yu and X. Liang, *J. Alloys Compd.*, 2013, **562**, 176. (b) M. P. Saradhi and U. V. Varadaraju, *Chem. Mater.*, 2006, **18**, 5267.
20 (a) G. Blasse, *J. Solid State Chem.*, 1986, **62**, 207; (b) G. Blasse, *Phys. Lett. A*, 1968, **28**, 444; (c) C.-H. Huang, W.-R. Liu, T.-S. Chan and Y.-T. Lai, *Dalton Trans.*, 2014, **43**, 7917; (d) S.-P. Lee, C.-H. Huang and T.-M. Chen, *J. Mater. Chem. C*, 2014, **2**, 8925; (e) T.-C. Liu, H. Kominami, H. F. Greer, W. Zhou, Y. Nakanishi and R.-S. Liu, *Chem. Mater.*, 2012, **24**, 3486.
21 (a) S. J. Gwak, P. Arunkumar and W. B. Im, *J. Phys. Chem. C*, 2014, **118**, 2686; (b) W. Xiao, X. Zhang, Z. Hao, G.-H. Pan, Y. Luo, L. Zhang and J. Zhang, *Inorg. Chem.*, 2015, **54**, 3189; (c) L. G. Van Uitert, *J. Electrochem. Soc.*, 1967, 114, 1048; (d) D. L. Dexter, *J. Chem. Phys.*, 1953, **21**(5), 836.
22 E. Pavitra, G. S. R. Raju, Y. H. Ko and J. S. Yu, *Phys. Chem. Chem. Phys.*, 2012, **14**, 11296.
23 (a) L. S. Wang, X. M. Liu, Z. W. Quan, D. Y. Kong, J. Yang and J. Lin, *J. Lumin.*, 2007, **122-123**, 36; (b) O. L. Malta, H. F. Vrito, J. F. S. Menezes, F. R. G. Silve, S. Alves and F. S. Farias, *J. Lumin.*, 1997, **75**(3), 255.
24 D. L. Dexter, *J. Chem. Phys.*, 2004, **21**, 836.
25 (a) P. I. Paulose, G. Jose, V. Thomas, N. V. Unnikrishnan and M. K. R. Warrier, *J. Phys. Chem. Solids*, 2003, **64**, 841; (b) N. Xie , J. Liu, Y. Huang , S. Kim and H. J. Seo, *Ceram. Inter.*, 2012, **38**, 1489.
26 D. L. Dexter and J. H. Schulman, *J. Chem. Phys.*, 1954, **22**, 1063.
27 (a) J. Chen, Y. Liu, M. Fang and Z. Huang, *Inorg. Chem.*, 2014, **53**, 11396; (b) H. P. You, J. L. Zhang, G. Y. Hong and H. J. Zhang, *J.* Phys. *Chem.* C, 2007, **111**, 10657.
28 J. M. P. J. Verstegen, J. L. Sommerdijk and J. G. Verriet, *J. Lumin.*, 1973, **6**, 425.
29 (a) J. S. Kim, Y. H. Park, S. M. Kim, J. C. Choi and H. L. Park, Solid State *Commun.*, 2005, **133**, 445; (b) D. Hsu and J. L. Skinner, *J. Chem. Phys.*, 1984, **81**, 5471.
30 (a) M. Xin, D. Tu, H. Zhu, W. Luo, Z. Liu, P. Huang, R. Li, Y. Cao and X. Chen, *J. Mater. Chem. C*, 2015, **3**, 7286; (b) X. Zhang, J. Wang, L. Huang, F. Pan, Y. Chen, B. Lei, M. Peng and M. Wu, *ACS Appl. Mater. Interface*, 2015, **7** (18), 10044; (c) X. Zhang, L. Huang, F. Pan, M. Wu, J. Wang, Y. Chen and Q. Su, *ACS Appl. Mater. Interface*, 2014, **6** (4), 2709.

View Article Online
DOI: 10.1039/C5TC01993A



# TOC Graphic

A series of tunable blue-green to white phosphors $Sr_2Y_8(SiO_4)_6O_2:Bi^{3+}$, $Eu^{3+}$ phosphors prepared via Pechini-type sol-gel method have been investigated.